Journal of Applied Phycology (2020) 32:1243–1251
https://doi.org/10.1007/s10811-020-02048-w

Solar UV radiation exacerbates photoinhibition of a diatom by antifouling agents Irgarol 1051 and diuron

Rui Hou[1] · Yaping Wu[1,2] · Juntian Xu[2] · Kunshan Gao[3]

Received: 16 October 2019 / Revised and accepted: 20 January 2020 / Published online: 4 February 2020

Abstract

Marine diatoms are ubiquitously distributed in both coastal and open oceans, playing an important role in global primary productivity. In coastal waters, they are exposed to various pollutants in addition to multiple environmental stressors. Here, we show the pennate diatom *Nitzschia* sp. isolated from the East China Sea decreased its photosynthetic performance under the combined influences of two typical marine organic pollutants (Irgarol 1051 and diuron), that are frequently used as biocides to prevent biofouling, and solar UV radiation (UVR). *Nitzschia* sp. was sensitive to both pollutants under visible light (PAR) without UVR, even at the lowest concentration (0.5 μg L^{-1}) tested; higher levels led to greater reductions in its photochemical yield. When additionally exposed to UVR (280–400 nm), the inhibition of the quantum yields by the antifouling pollutants was exacerbated, reflecting a synergistic impact of the pollutants and UVR. Exposure to UVR brought about 5–20% reduction at different levels of Irgarol 1051, diuron, and their mixture, with a higher reduction percentage due to UVR observed at lower concentrations of the pollutants. Our results indicate that even low levels of antifouling agents can result in significant impacts on diatoms in the presence of solar UVR, implying that combinations of UVR and organic pollutants could be a potential method to control-target algal biofouling.

Keywords Antifouling biocides · *Nitzschia* · Photoinhibition · UV radiation

Introduction

The East China Sea is an important carbon sink region (Gao and Song 2006); therefore, variations of primary production in this region have been a strong focus of research in past decades (Liu et al. 2010). Under the influence of riverine input from the Yangtze river, the chemical and physical environment of this estuarine area is very complex; e.g., influencing salinity regimes, the riverine water carries various chemicals, including nutrients, herbicides, and heavy metals (Wang et al. 2011). The main phytoplankton groups in the estuary and adjacent waters of the Yangtze river are diatoms and dinoflagellates (Zhu et al. 2009). The community structure of phytoplankton exhibits typical regional distribution characteristics, with diatoms and chlorophytes contributing large fractions of the communities in nearshore waters, while dinoflagellates account for up to 82.7% in the offshore areas (Gao and Song 2005).

The microalgae comprising the phytoplankton are the main primary producers in the ocean (Klais et al. 2015), and diatoms contribute about 40% to marine primary productivity (Carstensen et al. 2015). The contrasting phytoplankton populations' characteristic of different niches may reflect species or population-specific strategies to adapt to different regional environments (Cerino et al. 2005; Barnett et al. 2015). Microalgae can also adhere onto the natural or artificial surface and create biofilms within a few days (Landoulsi et al. 2011). These can lead to increased friction and fuel consumption for ships, e.g., a 1-mm thick layer of biofouling algae has been suggested to increase hull friction by 80% and lead to

Electronic supplementary material The online version of this article (https://doi.org/10.1007/s10811-020-02048-w) contains supplementary material, which is available to authorized users.

✉ Yaping Wu
ypwu@jou.edu.cn

[1] Institute of Marine Biology, College of Oceanography, Hohai University, Nanjing 210098, China

[2] College of Marine Life and Fisheries, Jiangsu Ocean University, Lianyungang 222005, China

[3] State Key Laboratory of Marine Environmental Science, Xiamen University, Xiamen 361005, China

increased fuel consumption by 17% (Evans et al. 2000). Therefore, antifouling paints are frequently used to prevent the biofouling on artificial surfaces (Zamora-Ley et al. 2006; Gallucci et al. 2015).

Tributyltin was one of the most commonly used antifouling agents. However, this compound is highly toxic to nontarget organisms, and has been prohibited for commercial use since 2003 (Yebra et al. 2004; Turner 2010). Subsequently, Irgarol 1051 has now become one of the most common antifouling paint biocides (Buma et al. 2009; Hirayama et al. 2017). The primary target of this compound is the proteins that carry electrons within photosystem II (PSII), acting to interrupt the electron transport and thereby inhibit the growth of algae on artificial surfaces (Ansanelli et al. 2017). However, these compounds leach into the water body and can potentially cause problems. In the coastal waters of Singapore; for instance, Irgarol 1051 concentrations can reach as much as 4.2 μg L^{-1}, levels that are sufficient to influence photoautotrophs in seawater (Basheer et al. 2002; Kottuparambil et al. 2017). In addition, the discharged waters from land carry herbicides such as diuron, a predominant chemical used for weed control, which is also an inhibitor of PSII (Gatidou and Thomaidis 2007); hence, phytoplankton could be exposed to both toxic chemicals in estuarine areas. However, little has been documented on distribution and impacts of antifouling chemicals in the Yangtze river and the adjacent waters, where global shipping industry is active.

As an important physical driver, light potentially modulates the toxicity of organic pollutants to photoautotrophs. Previous studies have revealed that dynamic light or light history (without UVR) could alter the sensitivity of biofilms to pollutants (Laviale et al. 2010; Bonnineau et al. 2012). As UVR is the most energetic waveband within the sunlight spectrum reaching the earth's surface, it is likely that this should have a more intense interaction with other chemical drivers (Barnes et al. 2019); e.g., UVR synergistically reduces the photosynthetic activity of diatoms under high salinity or in the presence of copper (Wu et al. 2017; Zhu et al. 2019). Possible interactions of UVR with organic pollutants such as Irgarol and diuron are, however, still unknown (Lambert et al. 2006). In estuarine areas, pennate diatoms play an important role in the generation of biofilms, which provide suitable microenvironment for bacterial community succession on ship's surface (Landoulsi et al. 2011). In addition, they are also resuspended frequently by turbulence, and can then contribute a substantial fraction to primary production in the water column (Underwood et al. 1998). Considering the widespread distribution of Irgarol 1051 and diuron in natural seawater, and their similar primary target sites on photosystem II, we isolated *Nitzschia* sp. from the estuary of the Yangtze river to test the hypothesis that these two pollutants could interactively affect the photochemical process of pennate diatoms, particularly under the influence of UVR.

Materials and methods

Algal culture

The diatom *Nitzschia* sp. was isolated from the estuary of the Yangtze river in June 2018 and maintained in a growth chamber under 50 μmol photons m^{-2} s^{-1} and 20 °C. Before the experiment, this diatom was inoculated into 500 mL polycarbonate bottles filled with 400 mL sterilized natural seawater and enriched with F/2 medium, with a starting cell concentration of 500 cells mL^{-1}. The bottles were placed in an incubator, with light intensity around 150 μmol photon m^{-2} s^{-1} under a 12/12 light/dark cycle, while temperature was controlled at 20 °C. Triplicate cultures for each treatment were maintained at exponential phase by semi-continuously diluting with fresh medium every 24 h, maintaining the cell concentrations below ~ 2×10^4 cells mL^{-1}, while bottles were manually shaken 3–4 times every day.

Test chemicals and solution

Known amounts of 2-(tert-butylamino)-4-(cyclopropylamino)-6-(methylthio)-s-triazine (Irgarol 1051) and diuron were weighed and dissolved in DMSO (dimethyl sulfoxide) to a final concentration of 1 μg mL^{-1}. In addition, lincomycin, which is a frequently used chemical to block protein synthesis within the chloroplast, was prepared to determine the damage rate of photosystem II in the absence of repair processes.

Experimental setup

During the light exposure, a solar simulator with a 1000 W xenon lamp (Ji Guang Inc. China) was used as the light source, and the light intensity was adjusted by altering the distance between xenon lamp and the water bath. The intensity of PAR (400–700 nm), UVA (315–400 nm), and UVB (280–315 nm) was measured by a light meter (PMA2100, Solar Light Inc.), and values were 470 μmol photons m^{-2} s^{-1}, 12.2 W m^{-2}, and 2.84 W m^{-2}, respectively.

The culture of *Nitzschia* sp. was sampled during the middle of the light period, and dispensed into 50 mL quartz tubes, and then the pollutants (Irgarol 1051, diuron, or lincomycin) added to final concentrations of 0.5, 1.0, and 2.0 μg L^{-1} for the determination of the independent effect of each pollutant; the same volume of DMSO was added to the control. To investigate the potential interactive effects between pollutants, equal concentrations of Irgarol 1051 and diuron were added to the samples, with the same total final concentration as above. In addition, a parallel experiment with a final concentration of 0.5 mg mL^{-1} lincomycin (which fully blocked the repair process within PSII) was conducted, to determine the damage rate under the respective light treatments.

After the addition of pollutants under light, the quartz tubes were placed in a water bath, underneath a cutoff filter (ZJB280 for PAB [PAR + UV-A + UV-B] treatment and ZJB400 for P [PAR] treatment) (Yin Xing Inc. China), while temperature was controlled at 20 °C by a chiller (CTP3000, Eyela, Japan). A subsample (2 mL) was immediately withdrawn for measurement of initial chlorophyll fluorescence, and subsequent measurements were conducted at specific time intervals (see below). After 60-min exposure, the quartz tubes were moved into another water bath (20 °C) under dim light (~ 20 μmol photons m^{-2} s^{-1}) for recovery (~ 80 min), and fluorescence was then measured again.

Chlorophyll fluorescence measurements

Due to the space limitation under the solar simulator, we performed each experiment with 6 quartz tubes (2 pollutants under 1 light regime). Since the cultures were maintained in exponential phase by semi-continuous dilution, all samples were in a similar physiological state (as shown in the initial fluorescence yield values) before the measurements. During the experiment, 2 mL of sample was taken to measure the effective quantum yield with an AquaPen fluorometer (AP-C 100, PSI, Czech Republic). After a total of 7 rounds of measurement (60 min), tubes were transferred into a low-light environment under the same temperature for recovery, and effective quantum yield was measured for the next 80 min.

Data analysis

The effective quantum yield (EQY) measured with the AquaPen was calculated as follows:

$$\mathrm{EQY} = (\mathrm{F_m}' - \mathrm{F_o}')/\mathrm{F_m}',$$

where F_m' is the maximum effective fluorescence in the presence of actinic light and F_0' is the minimum fluorescence measured with a modulated measuring light (0.01 μmol photons m^{-2} s^{-1}) under incubation light. To have a better comparison among treatments, the EQY was converted to relative values, with initial values set as 1 at time zero, and all subsequent values were normalized as relative quantum yield (RQY) accordingly.

The damage rate to PSII caused by UVR (k, min^{-1}) and repair rate (r, min^{-1}) were fitted to the Kok equation:

$$\frac{Pt}{Po} = \frac{r}{k+r} + \frac{k}{k+r} e^{-(k+r)t}$$

where P_o is the EQY at time zero under incubation light, and P_t is the EQY at time t (min). First, k values under P and PAB treatments were obtained in the presence of 0.5 mg mL^{-1} lincomycin (which fully blocked the protein repair in PSII), while r values for lincomycin-free samples were obtained from the determined k value through the Kok equation.

To determine the recovery rate of the high light–damaged cells during subsequent exposure to dim light, mimicking the movement in nature of cells from the surface to deep water by mixing, the rate constant of recovery (min^{-1}) was then calculated by an exponential rise equation:

$$\mathrm{y} = y_0 + c(1 - e^{-\alpha t}),$$

where y is the EQY at time t (min) in the dim light recovery experiment, y_0 and c are constants, and α is the rate constant of recovery (min^{-1}) (Heraud and Beardall 2000).

The relative pollutant inhibition of EQY was calculated by the following equation:

$$\text{Relative pollutant inhibition} = (P_c - P_R)/P_c$$

where P_R represents EQY when samples were exposed to the pollutant (Lincomycin, Irgarol 1051, diuron, or Irgarol 1051 & diuron) and P_C represents EQY of the control treatment to which only the solvent DMSO had been added.

A two-way repeated measures ANOVA was used to analyze the impact of independent effects and the interactions of radiation and pollutant, while significance among different levels of pollutants were assessed with a Turkey post hoc test.

Results

Under the P treatment, the RQY of the control treatment decreased quickly to ~ 80% of the initial value after 6 min under the solar simulator and remained stable during the rest of the exposure (Fig. 1a). However, the RQY of samples that were treated with Irgarol 1051 decreased steadily to the end of the light exposure, with the lowest value observed for samples treated with 2 μg L^{-1} Irgarol 1051, around 50% of initial value. Significant differences were observed among the 3 levels of Irgarol 1051 ($p < 0.001$, Table 1). For samples to which diuron was added, the RQY quickly decreased and reached a stable value within 12 min, around 70% of initial value, but the amplitude of the decrease was smaller than under the Irgarol 1051 treatments. The differences among the 3 levels of diuron tested were significant (Fig. 1b) ($p < 0.05$, Table 1). After the addition of the mixture of Irgarol 1051 and diuron, the RQY showed a similar pattern, with values decreasing to the end of the light exposure, around 56% of initial value. However, the difference between 0.5 and 1 μg L^{-1} was insignificant (Fig. 1c, Table 1). During the dim light incubation, the control samples recovered quickly to the initial value within 10 min, while the other samples treated with Irgarol 1051, diuron or their mixture recovered much slower and reached ~ 70, ~ 90, and ~ 70% of the initial value after 80 min, respectively (Fig. 1a, b, and c).

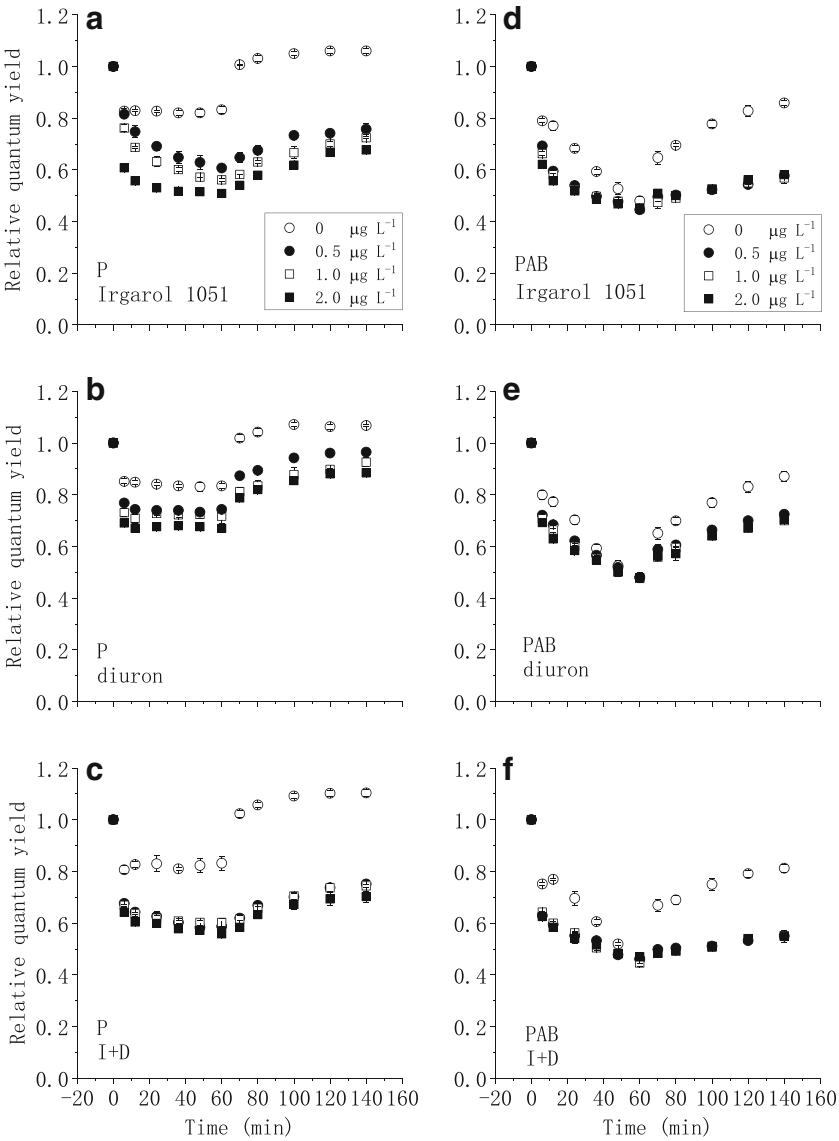

Fig. 1 The RQY of *Nitzschia* sp. for 60 min light exposure and subsequent recovery under dim light for 80 min, which added Irgarol 1051 (**a**), diuron (**b**), or Irgarol 1051 + diuron (**c**) under P (PAR) treatment, and Irgarol 1051 (**d**), diuron (**e**), or Irgarol 1051 + diuron (**f**) under PAB (PAR + UV-A + B) treatment. Vertical lines represent SD, $n = 3$

Under the PAB treatment, the RQY decreased quickly after 6-min exposure, with a slower rate for the control group than for those groups to which the pollutants had been added; values were also significantly higher at the start of the 30-min exposure. Subsequently, samples with added pollutants approached equilibrium, while the control group still continued decreasing, resulting in comparable values for RQY of around 45% of the initial value for all treatments at the end of the PAB exposure (Fig. 1d, e, and f). Among 3 levels of Irgarol 1051, the highest level treatment (2.0 μg L^{-1}) had the lowest quantum yield than the other level treatments ($p < 0.05$, Table 1) (Fig. 1d). When diuron or the mixture of Irgarol 1051 and diuron were added, RQY values were significantly lower than in the control group ($p < 0.001$, Table 1), while no significant differences among the 3 levels of pollutant treatments were found (Fig. 1e and f, Table 1). For treatments that included pollutants and UVR, RM-ANOVA results showed that there were significant interactions between UVR and the two tested pollutants or their mixture (Table 2). During the dim light incubation, the control sample recovered quickly to about 86% of the initial value within 80 min, while the samples with added with Irgarol 1051, diuron or the mixture could only recover to about 56, 70, and 55% of the initial value, respectively (Fig. 1d, e, and f).

During the light exposure, the EQY ratio between values at the lowest level and highest level of pollutant was associated with the radiation treatments; values of Irgarol 1051-treated cells were ~ 1.20 under the P treatment, but significantly decreased to ~ 1.03 under the PAB treatment. The, diuron- or mixture-treated cells generally had lower values than cells under the Irgarol treatment under *P*, with ratios ranging from 1.05–1.10, though these were still significantly higher than under the PAB treatment, which almost decreased to 1.0 (Fig. 2b and c).

Table 1 The statistical results (p value) of post hoc test for the comparison among different levels of pollutants during the light exposure, the bold numbers indicate no significant differences ($p > 0.05$)

Treatments Pollutant Concentration (μg L^{-1})		Irgarol		Diuron		I + D	
		P	PAB	P	PAB	P	PAB
0.0	0.5	0.000	0.000	0.000	0.004	0.000	0.000
	1.0	0.000	0.000	0.000	0.001	0.000	0.000
	2.0	0.000	0.000	0.000	0.000	0.000	0.000
0.5	0.0	0.000	0.000	0.000	0.004	0.000	0.000
	1.0	0.001	0.325	0.042	0.406	0.978	0.991
	2.0	0.000	0.003	0.000	0.079	0.034	0.844
1.0	0.0	0.000	0.000	0.000	0.001	0.000	0.000
	0.5	0.001	0.325	0.042	0.406	0.978	0.991
	2.0	0.000	0.032	0.001	0.627	0.020	0.949
2.0	0.0	0.000	0.000	0.000	0.000	0.000	0.000
	0.5	0.000	0.003	0.000	0.079	0.034	0.844
	1.0	0.000	0.032	0.001	0.627	0.020	0.949

During the light exposure and dim light incubation, the repair rate, damage rate of PSII, and rate constant for recovery were fitted from the kinetics of RQY. The repair rate was about 0.065 min^{-1} for cells that were treated with 0.5 μg L^{-1} diuron under the P treatment, while much lower values were observed for the Irgarol 1051 treated samples (~ 0.04 min^{-1}) or mixed pollutants (0.03 min^{-1}) (Fig. 3a). Those repair rates decreased further when exposed to UVR (Fig. 3b). The corresponding damage rates were around 0.025 and 0.038 min^{-1} for P and PAB treatments, respectively (Fig. 3a and b). During the dim light incubation after PAR exposure, the rate constants for recovery of the control group was much higher than for samples with added pollutants, while samples with Irgarol 1051 or the mixture were significantly lower than for the diuron alone treatment (Fig. 3c). The overall pattern of rate constants for recovery under PAB treatment was similar to that in the P treatment, while absolute values were much lower (Fig. 3d).

The addition of pollutants also induced significant inhibition on PSII, while the changing pattern was associated with the light regime to which the cells were exposed. Under the P treatment, the relative Irgarol 1051 inhibition increased and

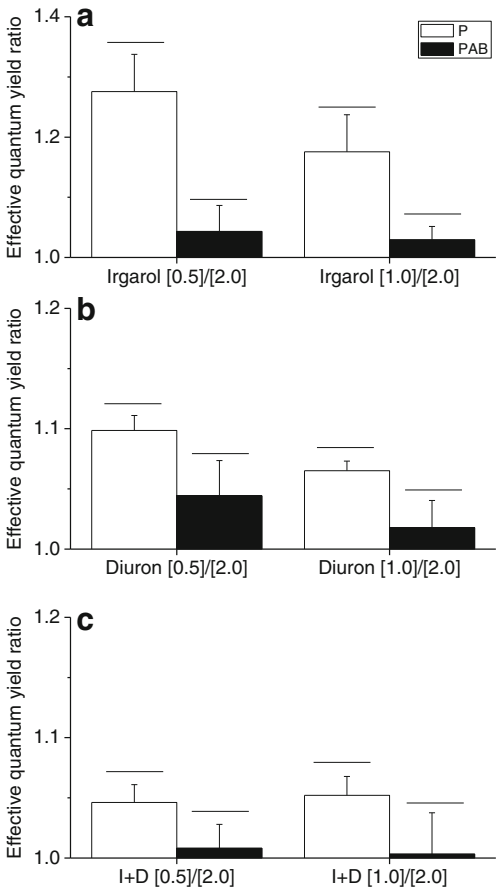

Fig. 2 The effective quantum yield (EQY) ratios of low-levels (0.5 or 1.0 μg L^{-1}) to the highest level pollutant (2.0 μg L^{-1})-treated cells under P or PAB treatment, Irgarol 1051 treated (**a**), diuron treated (**b**), mixture (Irgarol 1051 + diuron) treated cells (**c**). Horizontal lines indicate significant difference between treatments, vertical lines represent SD, $n = 6$

reached its highest value at the end of exposure, up to ~ 38% at a concentration of 2.0 μg L^{-1} (Fig. 4a). However, the relative Irgarol 1051 inhibition exhibited a different pattern under PAB treatment; in that, it increased in the first 12 min but decreased toward the end of the light exposure (Fig. 4b). Similar patterns were observed for samples exposed to diuron or the mixture, while the highest inhibitions observed were ~ 20 and 15% for diuron and 33% and 24% for the mixture under P or PAB treatments, respectively (Fig. 4c, d, e, and f). Moreover, the

Table 2 The statistical results of RM-ANOVA for effective quantum yield during light exposure under different pollutants and radiation treatments

Pollutants Factors	Irgarol			diuron			I + D		
	df	F	p	df	F	p	df	F	p
Time	6	6775.03	0.000	6	5865.61	0.000	6	6325.50	0.000
Time*radiation	6	223.73	0.000	6	867.11	0.000	6	305.56	0.000
Time*pollutant	18	93.60	0.000	18	43.97	0.000	18	66.66	0.000
Time*radiation*pollutant	18	60.69	0.000	18	13.97	0.000	18	40.44	0.000

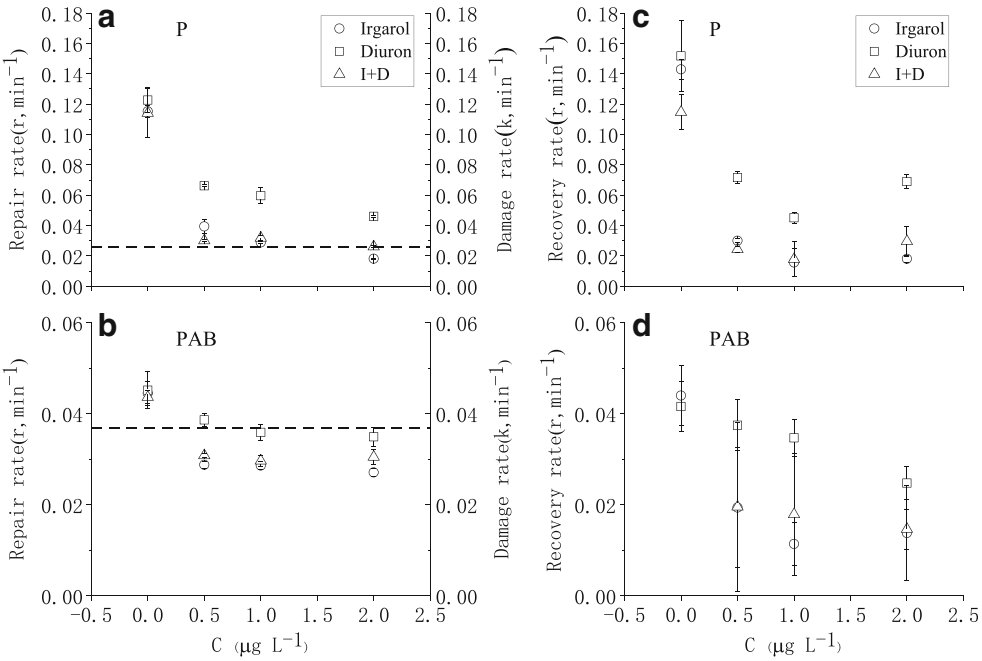

Fig. 3 The repair rate of photosystem II in *Nitzschia* sp. during PAR (**a**) or PAB (**b**) exposure with different pollutants, and the corresponding rate constant for recovery during subsequent dim light incubation (**c**, **d**). The dotted line represents the damage rate under respective light treatment. Vertical lines represent SD, $n = 3$

relative inhibition was correlated with pollutant concentration, with, in general, higher level of pollutants inducing higher inhibition of PSII, particularly for cells exposed to PAR, with larger differences among different levels for Irgarol 1051- and diuron-treated cells.

Discussion

Under the influence of human activities, coastal oceans have been becoming more vulnerable due to progressively increased of riverine inputs of inorganic and organic compounds, many of which are pollutants, causing a series of environmental risks, e.g., algal bloom, hypoxia, etc. (Wang et al. 2017). Therefore, the widely distributed toxic chemicals found around the world, e.g., pesticides, heavy metals, and antifouling paints, potentially threaten the health of coastal ecosystems (Connelly et al. 2001; Ali et al. 2013). *Nitzschia* belongs to a commonly found group of pennate diatoms that contains species that are potentially toxic, which account for substantial primary production in estuary area (Bates et al. 2018). In the present work, both Irgarol 1051 and diuron had significant inhibitory effects on the photochemistry of *Nitzschia* sp., even at low concentrations, and UVR exacerbated the photoinhibition, indicating a synergistic impact of the anti-biofouling and UVR. Our results suggest that the threshold of effects of typical organic pollutants could be lower with impacts of UVR being included.

Although many chemicals are effective at preventing fouling on paint surfaces, most of them are toxic enough to affect bacteria and crustaceans, and misuse of them could threaten nontarget organisms (Soroldoni et al. 2017). The predominant antifouling chemical, Irgarol 1051, is a triazine antifouling agent that targets the D1 protein in PSII of primary producers (Owen et al. 2002), while diuron is a phenylurea herbicide, which can inhibit the Hill reaction in photosynthesis (Jones and Kerswell 2003). Therefore, both agents could have potential synergistic impacts on photoautotrophs (Kottuparambil et al. 2017). However, environmental risk assessments usually focus on a single compound, but the natural water and organisms are often affected by mixed pollutants and other environmental factors. Microalgae are likely be affected synergistically (Gatidou and Thomaidis 2007), while seagrass showed higher resistance to mixed pollutants (Diepens et al. 2017).

As the first step in photosynthesis, the photochemical process is very sensitive to environmental factors (McCarthy et al. 2012; Zhu et al. 2019), in which light is the most effective factor that mediates the performance of photosystems (Key et al. 2010). We have shown here that under high light stress, the relative quantum yield decreased, the extent of which was dependent on the levels of the pollutants (Fig. 1). The highest level of Irgarol 1051 or diuron reduced relative quantum yield more than lower levels under P treatment, while when Irgarol 1051 and diuron were added together, even the lowest level of both could result in similar inhibitory effects as the highest one of each, indicating a synergistic effect of these two pollutants (Fig. 1c). Moreover, there were significant interactions between the pollutants and UVR, particularly at low concentration (Fig. 2); that is, the presence of UVR exacerbated the harmful effects of the pollutants. This indicates that toxicity of pollutants

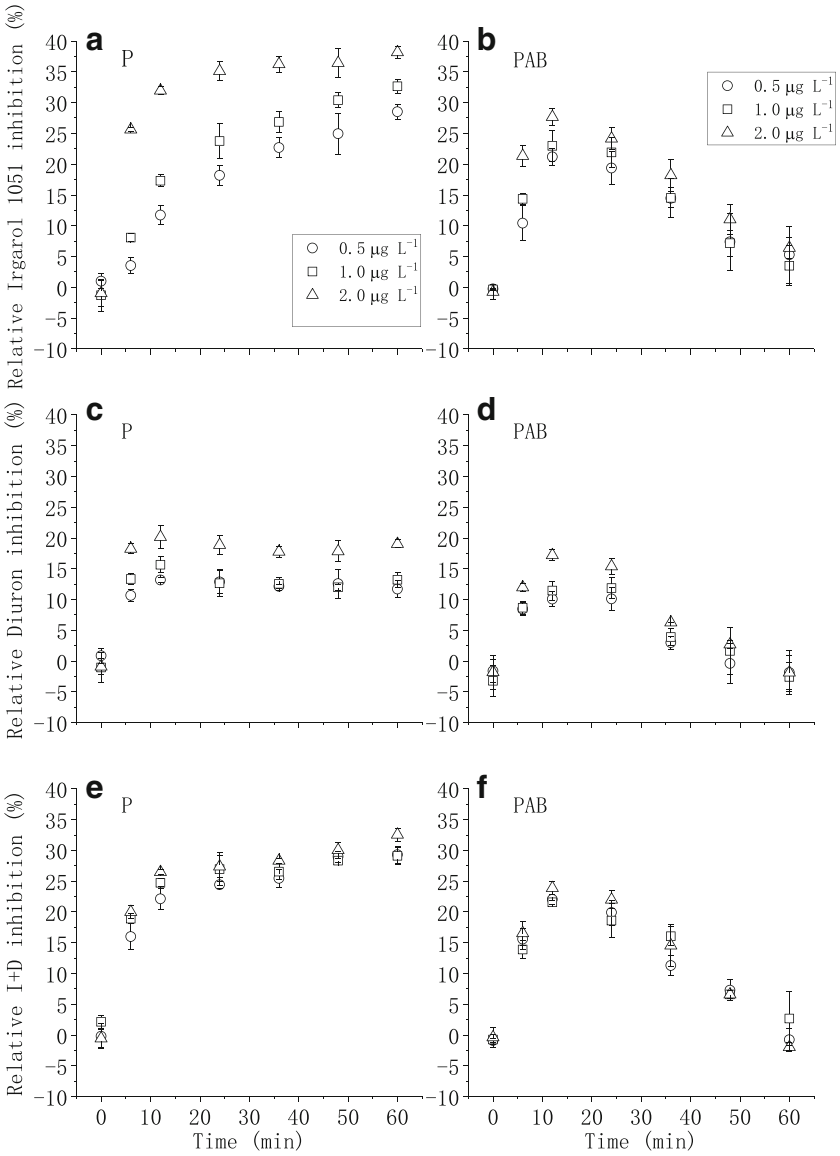

Fig. 4 The relative inhibition of pollutants (Irgarol 1051, diuron, or mixture [I + D]) on the photosystem II of *Nitzschia* sp. under P or PAB treatment. Vertical lines represent SD, $n = 3$

would be higher than expected before under the influence of multiple environmental stressors, such as UV.

Some diatoms, brown algae and cyanobacteria are known to show tolerance to diuron (Magnusson et al. 2012) or Irgarol 1051 (Eriksson et al. 2009), and the impacts of these pollutants on the algae seem to be reversible; when pre-treated cells are reintroduced into fresh seawater, diuron can be "washed" from the Q_b site, giving a rise to the rapid recovery of photochemical efficiency. However, Irgarol 1051 behaved more persistent, continuously inhibiting the photosynthesis of phytoplankton (Buma et al. 2009), while for benthic diatoms involved in the creation of biofilms, their resistance to herbicides increased (Larras et al. 2013). In addition, the toxicity of degradation products sometimes is greater than their original source (Fernández-Alba et al. 2002), which needs to be taken into account when performing long-term toxicity test experiments.

In the past, most marine antifouling agents contained copper, while zinc oxide was often used as a booster that increases the antifouling potency of copper (Turner 2010). The newest antifouling products usually use at least 2 chemicals, i.e., Irgarol 1051 and diuron, to enhance the antifouling efficiency. Previous studies have shown that although the interaction between Irgarol 1051 and diuron was still unclear, indeed, the combination of those two chemicals at different concentrations has been shown to yield antagonistic, additive, or synergistic effects on marine algae (Chesworth et al. 2004; Kottuparambil et al. 2017). Considering their impacts in the euphotic zone, exposure to solar UVR could further aggravate the pollutant-induced stresses with which phytoplankton are confronted (Barnes et al. 2019). Our results support the previous findings that there was a synergistic effect between Irgarol 1051 and diuron (Fernández-Alba et al. 2002). Interestingly, our data also clearly showed that the presence of UVR greatly

amplified the impacts of Irgarol 1051at low concentration (Fig. 1d), resulting in comparable inhibition at the highest concentration (Fig. 4b). This implies that the inhibitory effects of Irgarol 1051 could be much higher if UVR effects are taken into account, and that may provide a new perspective, i.e., combination of UV radiation and organic compounds, for the control of biofouling algae (Yebra et al. 2004).

Though the emission of ozone-depleting substances was prohibited after the Montreal Protocol, the global development of industry still poses a potential threat to the atmosphere, and a recent report has shown that the emission of chlorofluorocarbons has not fully stopped; thus, photoautotrophs still have to cope with increased UV-B irradiance due to depletion of the ozone layer (Montzka et al. 2018). Ultimately, the anti-biofouling agents and solar UVR, along with other ocean global and regional changes, might interact to inhibit phytoplankton photosynthesis and primary productivity, thereby influencing ecosystem services (Okamura et al. 2000; Gao et al. 2019).

Acknowledgments We thank Professor John Beardall for his linguistic assistance.

Funding information This research was funded by Natural Science Foundation of Jiangsu Province of China (BK20181314), Natural Science Foundation of China (41876113). and the Fundamental Research Funds for the Central Universities (2019B18614).

References

Ali HR, Arifin MM, Sheikh MA, Mohamed Shazili NA, Bachok Z (2013) Occurrence and distribution of antifouling biocide Irgarol-1051 in coastal waters of peninsular Malaysia. Mar Pollut Bull 70: 253–257

Ansanelli G, Manzo S, Parrella L, Massanisso P, Chiavarini S, Di Landa G, Ubaldi C, Cannarsa S, Cremisini C (2017) Antifouling biocides (Irgarol, Diuron and dichlofluanid) along the Italian Tyrrhenian coast: temporal, seasonal and spatial threats. Reg Stud Mar Sci 16: 254–266

Barnes PW, Williamson CE, Lucas RM, Robinson SA, Madronich S, Paul ND, Bornman JF, Bais AF, Sulzberger B, Wilson SR, Andrady AL, McKenzie RL, Neale PJ, Austin AT, Bernhard GH, Solomon KR, Neale RE, Young PJ, Norval M, Rhodes LE, Hylander S, Rose KC, Longstreth J, Aucamp PJ, Ballaré CL, Cory RM, Flint SD, de Gruijl FR, Häder D-P, Heikkilä AM, Jansen MAK, Pandey KK, Robson TM, Sinclair CA, Wängberg S-Å, Worrest RC, Yazar S, Young AR, Zepp RG (2019) Ozone depletion, ultraviolet radiation, climate change and prospects for a sustainable future. Nature Sustainability 2:569–579

Barnett A, Meleder V, Blommaert L, Lepetit B, Gaudin P, Vyverman W, Sabbe K, Dupuy C, Lavaud J (2015) Growth form defines physiological photoprotective capacity in intertidal benthic diatoms. ISME J 9:32–45

Basheer C, Tan KS, Lee HK (2002) Organotin and Irgarol-1051 contamination in Singapore coastal waters. Mar Pollut Bull 44:697–703

Bates SS, Hubbard KA, Lundholm N, Montresor M, Leaw CP (2018) Pseudo-nitzschia, Nitzschia, and domoic acid: new research since 2011. Harmful Algae 79:3–43

Bonnineau C, Sague IG, Urrea G, Guasch H (2012) Light history modulates antioxidant and photosynthetic responses of biofilms to both natural (light) and chemical (herbicides) stressors. Ecotoxicology 21:1208–1224

Buma AGJ, Sjollema SB, van de Poll WH, Klamer HJC, Bakker JF (2009) Impact of the antifouling agent Irgarol 1051 on marine phytoplankton species. J Sea Res 61:133–139

Carstensen J, Klais R, Cloern JE (2015) Phytoplankton blooms in estuarine and coastal waters: seasonal patterns and key species. Estuar Coast Shelf Sci 162:98–109

Cerino F, Orsini L, Sarno D, Dell'Aversano C, Tartaglione L, Zingone A (2005) The alternation of different morphotypes in the seasonal cycle of the toxic diatom *Pseudo-nitzschia galaxiae*. Harmful Algae 4: 33–48

Chesworth JC, Donkin ME, Brown MT (2004) The interactive effects of the antifouling herbicides Irgarol 1051 and Diuron on the seagrass *Zostera marina* (L.). Aquat Toxicol 66:293–305

Connelly DP, Readman JW, Knap AH, Davies J (2001) Contamination of the coastal waters of Bermuda by organotins and the triazine herbicide Irgarol 1051. Mar Pollut Bull 42:409–414

Diepens NJ, Buffan-Dubau E, Budzinski H, Kallerhoff J, Merlina G, Silvestre J, Auby I, Nathalie T, Elger A (2017) Toxicity effects of an environmental realistic herbicide mixture on the seagrass *Zostera noltei*. Environ Pollut 222:393–403

Eriksson KM, Clarke AK, Franzen LG, Kuylenstierna M, Martinez K, Blanck H (2009) Community-level analysis of *psbA* gene sequences and Irgarol tolerance in marine periphyton. Appl Environ Microbiol 75:897–906

Evans SM, Birchenough AC, Brancatoà MS (2000) The TBT ban: out of the frying pan into the fire? Mar Pollut Bull 40:204–211

Fernández-Alba AR, Hernando MD, Piedra L, Chisti Y (2002) Toxicity evaluation of single and mixed antifouling biocides measured with acute toxicity bioassays. Anal Chim Acta:303–312

Gallucci F, Castro IB, Perina FC, Souza Abessa DM, Paula Teixeira A (2015) Ecological effects of Irgarol 1051 and Diuron on a coastal meiobenthic community: a laboratory microcosm experiment. Ecol Indic 58:21–31

Gao X, Song J (2005) Phytoplankton distributions and their relationship with the environment in the Changjiang Estuary, China. Mar Pollut Bull 50:327–335

Gao X, Song J (2006) Main geochemical characteristics and key biogeochemical carbon processes in the East China Sea. J Coast Res 226: 1330–1339

Gao K, Beardall J, Häder D-P, Hall-Spencer JM, Gao G, Hutchins DA (2019) Effects of ocean acidification on marine photosynthetic organisms under the concurrent influences of warming, UV radiation, and deoxygenation. Front Mar Sci 6

Gatidou G, Thomaidis NS (2007) Evaluation of single and joint toxic effects of two antifouling biocides, their main metabolites and copper using phytoplankton bioassays. Aquat Toxicol 85:184–191

Heraud P, Beardall J (2000) Changes in chlorophyll fluorescence during exposure of *Dunaliella tertiolecta* to UV radiation indicate a dynamic interaction between damage and repair processes. Photosynth Res 63:123–134

Hirayama K, Takayama K, Haruta S, Ishibashi H, Takeuchi I (2017) Effect of low concentrations of Irgarol 1051 on RGB (R, red; G, green; B, blue) colour values of the hard-coral *Acropora tenuis*. Mar Pollut Bull 124:678–686

Jones RJ, Kerswell AP (2003) Phytotoxicity of photosystem II (PSII) herbicides to coral. Mar Ecol Prog Ser 261:149–159

Key T, McCarthy A, Campbell DA, Six C, Roy S, Finkel ZV (2010) Cell size trade-offs govern light exploitation strategies in marine phytoplankton. Environ Microbiol 12:95–104

Klais R, Cloern JE, Harrison PJ (2015) Resolving variability of phytoplankton species composition and blooms in coastal ecosystems. Estuar Coast Shelf S 162:4–6

Kottuparambil S, Brown MT, Park J, Choi S, Lee H, Choi H-G, Depuydt S, Han T (2017) Comparative assessment of single and joint effects of diuron and Irgarol 1051 on Arctic and temperate microalgae using chlorophyll a fluorescence imaging. Ecol Indic 76:304–316

Lambert SJ, Thomas KV, Davy AJ (2006) Assessment of the risk posed by the antifouling booster biocides Irgarol 1051 and diuron to freshwater macrophytes. Chemosphere 63:734–743

Landoulsi J, Cooksey KE, Dupres V (2011) Review – interactions between diatoms and stainless steel: focus on biofouling and biocorrosion. Biofouling 27:1105–1124

Larras F, Montuelle B, Bouchez A (2013) Assessment of toxicity thresholds in aquatic environments: does benthic growth of diatoms affect their exposure and sensitivity to herbicides? Sci Total Environ 463-464:469–477

Laviale M, Prygiel J, Créach A (2010) Light modulated toxicity of isoproturon toward natural stream periphyton photosynthesis: a comparison between constant and dynamic light conditions. Aquat Toxicol 97:334–342

Liu K-K, Chao S-Y, Lee H-J, Gong G-C, Teng Y-C (2010) Seasonal variation of primary productivity in the East China Sea: a numerical study based on coupled physical-biogeochemical model. Deep-Sea Res II 57:1762–1782

Magnusson M, Heimann K, Ridd M, Negri AP (2012) Chronic herbicide exposures affect the sensitivity and community structure of tropical benthic microalgae. Mar Pollut Bull 65:363–372

McCarthy A, Rogers SP, Duffy SJ, Campbell DA (2012) Elevated carbon dioxide differentially alters the photophysiology of *Thalassiosira pseudonana* (Bacillariophyceae) and *Emiliania huxleyi* (Haptophyta). J Phycol 48:635–646

Montzka SA, Dutton GS, Yu P, Ray E, Portmann RW, Daniel JS, Kuijpers L, Hall BD, Mondeel D, Siso C, Nance JD, Rigby M, Manning AJ, Hu L, Moore F, Miller BR, Elkins JW (2018) An unexpected and persistent increase in global emissions of ozone-depleting CFC-11. Nature 557:413–417

Okamura H, Aoyama I, Liu D, Maguire RJ, Pacepavicius GJ, Lau YL (2000) Fate and ecotoxicity of the new antifouling compound Irgarol 1051 in the aquatic environment. Water Res 34:3523–3530

Owen R, Knap A, Toaspern M, Carbery K (2002) Inhibition of coral photosynthesis by the antifouling herbicide Irgarol 1051. Mar Pollut Bull 44:623–632

Soroldoni S, Abreu F, Castro ÍB, Duarte FA, Pinho GLL (2017) Are antifouling paint particles a continuous source of toxic chemicals to the marine environment? J Hazard Mater 330:76–82

Turner A (2010) Marine pollution from antifouling paint particles. Mar Pollut Bull 60:159–171

Underwood GJC, Phillips J, Saunders K (1998) Distribution of estuarine benthic diatom species along salinity and nutrient gradients. Eur J Phycol 33:173–183

Wang L, Wang Y, Xu C, An Z, Wang S (2011) Analysis and evaluation of the source of heavy metals in water of the river Changjiang. Environ Monit Assess 173:301–313

Wang B, Chen J, Jin H, Li H, Huang D, Cai W-J (2017) Diatom bloom-derived bottom water hypoxia off the Changjiang Estuary, with and without typhoon influence. Limnol Oceanogr 62:1552–1569

Wu Y, Zhu Y, Xu J (2017) High salinity and UVR synergistically reduce the photosynthetic performance of an intertidal benthic diatom. Mar Environ Res 130:258–263

Yebra DM, Kiil S, Dam-Johansen K (2004) Antifouling technology—past, present and future steps towards efficient and environmentally friendly antifouling coatings. Prog Org Coat 50:75–104

Zamora-Ley IM, Gardinali PR, Jochem FJ (2006) Assessing the effects of Irgarol 1051 on marine phytoplankton populations in Key Largo Harbor, Florida. Mar Pollut Bull 52:935–941

Zhu Z-Y, Ng W-M, Liu S-M, Zhang J, Chen J-C, Wu Y (2009) Estuarine phytoplankton dynamics and shift of limiting factors: a study in the Changjiang (Yangtze River) estuary and adjacent area. Estuar Coast Shelf Sci 84:393-401

Zhu Z, Wu Y, Xu J, Beardall J (2019) High copper and UVR synergistically reduce the photochemical activity in the marine diatom *Skeletonema costatum*. J Photochem Photobiol B 192:97–102